Carbohydrate Polymers 86 (2011) 1799–1806

Contents lists available at ScienceDirect

Carbohydrate Polymers

journal homepage: www.elsevier.com/locate/carbpol

Coaxial electrospun poly(lactic acid)/chitosan (core/shell) composite nanofibers and their antibacterial activity

Thuy Thi Thu Nguyen [a], Ok Hee Chung [b], Jun Seo Park [a,*]

[a] Center of Chemical Technology and Division of Chemical Engineering, Hankyong National University, 167 Chungang-ro, Anseong-si, Gyeonggi-do 456-749, Republic of Korea
[b] Department of Physics, Sunchon National University, 413 Chungang-ro, Sunchon-si, Chunam-do 540-742, Republic of Korea

ARTICLE INFO

Article history:
Received 30 April 2011
Received in revised form 6 July 2011
Accepted 10 July 2011
Available online 19 July 2011

Keywords:
Coaxial electrospinning
Nanofibers
Chitosan
Poly(lactic acid)
Antibacterial

ABSTRACT

Biodegradable non-woven mats of poly(lactic acid) (PLA) and chitosan (CS) were fabricated by the coaxial electrospinning process. These non-woven mats are composed of PLA/CS core/shell composite nanofibers, in which PLA and CS form the core and shell layers, respectively. CS of high molecular weight could not be electrospun on its own because of its high viscosity in solution and its polycationic possession. The coaxial electrospinning method was able to facilitate the fabrication of double-layer PLA/CS composite nanofibers by employing a PLA layer in the core and a CS layer in the shell part. Transmission electron microscopy (TEM) studies and contact-angle measurements indicated the core/shell structure of the composite nanofibers fabricated with shell and core feed rates of 5 μL/min and less than 2 μL/min, respectively. The PLA/CS core/shell composite nanofibers showed antibacterial activity against *Escherichia coli*; hence it can be used as antibacterial materials in fields such as biomedical and filtration areas.

1. Introduction

Electrospinning is a versatile technique for the production of polymer fibers ranging from a few nanometers to several micrometers in diameter (Bhardwaj & Kundu, 2010; Frenot & Chronakis, 2003; Rutledge & Fridrikh, 2007). This is currently one of the most effective methods used in the manufacturing of high performance nanofibers with distinct specifications such as large surface-area-to-volume ratio and high porosity with small pore size (Chronakis, 2005). One further development of the electrospinning process is the technique of coaxial electrospinning (Ji et al., 2010; Liang, Hsiao, & Chu, 2007; Sun, Zussman, Yarin, Wendorff, & Greiner, et al., 2003). This method is capable of producing a continuous double layer of nanofibers by co-electrospinning two materials through a facile one-step procedure. Non-woven mat made through coaxial electrospinning can exhibit advantageous characteristics from each of the constituent materials. A non-woven nanofibrous fabric of polycarbonate (PC)/polyurethane (PU) core/shell composite nanofibers showed better morphology (with fewer beads) and better performance (better adhesion, higher mechanical strength) than the pure PC nanofibers (Sun et al., 2003). Double-layered composite nanofibers using biodegradable gelatin in the inner layer and another biodegradable poly(caprolactone) in the outer one was fabricated successfully (Huang, Zhang, & Ramakrishna, 2005). The tensile performance of these core/shell composite nanofibers was better than those of each of pure constituents. The possible applications of such nanofibers include drug release system, medical devices in the human body, utilizing their controllable degradation rate. Various drugs and bioactive agents such as antibiotics, DNA, proteins, or growth factors could be incorporated directly into the core, which was protected by the shell layer, and the results showed a sustained release of these agents from the non-woven mats of core/shell nanofibers over a long time period (He, Huang, & Han, 2009; Jiang et al., 2005; Jiang, Hu, Zhao, Li, & Zhu, 2006; Lu, Jiang, Tu, & Wang, 2009; Sill & von Recum, 2008; Xiaoqiang et al., 2009; Zhang et al., 2006). It was reported that some polymer solutions that are difficult to process could be co-electrospun to form ultrafine cores within the shells of other polymer materials. Although poly(glycerol sebacate) (PGS) is a rubbery polymer that could not be electrospun directly, the formation of PGS nanofibers was successfully achieved using the coaxial electrospinning process (Yi & LaVan, 2008).

Most biodegradable electrospun fibers such as chitosan, collagen, gelatin, hyaluronic acid, elastin, cellulose, and silk fibroin have been fabricated using single or blend biopolymers (Xie, Li, & Xia, 2008). Chitosan (CS), derived through the deacetylation of chitin, has aroused great interest as a new functional biomaterial because it possesses excellent biological properties such as biodegradability, biocompatibility, nontoxicity, antimicrobial activity, and wound-healing and scar-prevention properties (Jayakumar, Prabaharan, Sudheesh Kumar, Nair, & Tamura, 2011; Pillai, Paul, & Sharma, 2009). Electrospun CS nanofibers might have

* Corresponding author. Tel.: +82 31 670 5202; fax: +82 31 675 9604.
E-mail address: jspark@hknu.ac.kr (J.S. Park).

0144-8617/$ – see front matter © 2011 Elsevier Ltd. All rights reserved.
doi:10.1016/j.carbpol.2011.07.014

great potential in various fields including tissue engineering and wound dressing. However, the electrospinning of CS is extremely difficult because of its limited solubility in most organic solvents, its polycationic character in solution, its three-dimensional networks of strong hydrogen bonds, its high molecular weight, and its wide molecular weight distribution (Geng, Kwon, & Jang, 2005; Homayoni, Ravandi, & Valizadeh, 2009). The electrospinning ability of CS can be improved by blending it with other polymers that have good fiber-forming ability and good miscibility with CS. Several natural and synthetic polymers (such as cellulose, zein, poly(lactic acid), poly(caprolactone), Nylon-6, poly(vinyl alcohol), and so on) have been blended with CS to produce electrospun scaffolds with good mechanical properties (Jia et al., 2007; Shalumon et al., 2010; Shih, Shieh, & Twu, 2009; Torres-Giner, Ocio, & Lagaron, 2009; Xu et al., 2009; Zhang et al., 2009). Nevertheless, the electrospinning of these polymer blend solutions was difficult with high contents of CS in the blend. When the CS content in the blend with PVA was more than 30 wt%, nanofibers could hardly be formed (Jia et al., 2007). A fine morphology, without beads, of the electrospun CS/PLA blend nanofibers was obtained when the weight ratio of CS/PLA in the polymer blend was lower than 2/1 (Xu et al., 2009). Pure CS fibers have only been successfully electrospun at relatively low molecular weight using specific solvents, i.e., strong organic acids with low boiling points and low dielectric constants (Torres-Giner, Ocio, & Lagaron, 2008). Nanofibers of CS with a molecular weight of 210,000 g/mol were fabricated using triflouro-acetic acid as the solvent (Ohkawa, Cha, Kim, Nishida, & Yamamoto, 2004). Some studies on the electrospinning of CS with the use of concentrated acetic acid as the solvent have also been reported (Geng et al., 2005; Homayoni et al., 2009). CS with a molecular weight of 106,000 g/mol produced bead-free CS nanofibers, while that with a molecular weight of 398,000 g/mol did not. This may be because of the higher charge density of CS molecules containing more amino groups per molecule. CS can build into an electrospun scaffold through surface modifications such as simple coating, chemical reaction, plasma treatment, grafting, and so forth (Wang & Chen, 2005). The drawback of these methods is the relatively complicated fabrication process needed to attain the desired surface characteristics.

In this study, the coaxial electrospinning technique was used to produce PLA/CS core/shell composite nanofibers in which PLA and CS formed the core and the shell layer, respectively. PLA was chosen as a core material of coaxial electrospinning because of its excellent property such as non-toxic, strong mechanical strength, and good fiber-forming ability. CS of high molecular weight (690,000 g/mol, commercial grade) was used in the formation of the shell of PLA/CS core/shell composite nanofibers. As above-mentioned, high molecular weight of CS was unsuccessfully electrospun; hence, the employment of PLA in the core of nanofibers is expected to enhance the electrospinning ability of CS, and to improve mechanical strength of the nanofibers. Moreover, by coaxial electrospinning, CS as active component is all deposited on the surface of nanofibers which may show higher CS exposure than nanofibers fabricated by PLA/CS blend electrospinning. The effects of process parameters (such as the feed rate of the core) on the coaxial electrospinning process, the core/shell structure, and the fiber morphology were investigated. The structure of the core/shell composite nanofibers was confirmed by contact-angle measurements and transmission electron microscopy (TEM) observations. The morphology of the electrospun PLA/CS core/shell composite nanofibers was determined from field-emission scanning electron microscopy (FE-SEM) images. Differential scanning calorimetry (DSC) was conducted to investigate the composition of the nanofibers. The mechanical strength of the non-woven mat was evaluated with a tensile test. The potential application of these PLA/CS core/shell composite nanofibers as porous antibacterial materials was examined using antibacterial test.

2. Experimental

2.1. Materials

CS with a molecular weight of 690,000 g/mol and deacetylation degree of 90% was supplied by Biomaterials Co. (Korea). PLA with an average molecular weight of 200,000 g/mol (2002D-Grade) was supplied by NatureWorks Co. (USA). Acetic acid (glacial 99.5%), triflouro-acetic acid (TFA) (99.5%), and iodomethane were purchased from Samchun Co. (Korea). All the chemicals were used without further purification.

2.2. Coaxial electrospinning

CS (4 wt%) was dissolved in a mixture of acetic acid and TFA with a weight ratio of 10/90. TFA alone was used as the solvent for dissolving PLA at a concentration of 12 wt%. The coaxial spinneret consisted of two concentrically arranged capillaries. The inner capillary had inner and outer diameters of 0.35 mm and 0.65 mm, respectively, while the outer capillary had inner and outer diameters of 1.05 mm and 1.20 mm, respectively. Certain amounts of the PLA and CS solutions were contained in two individual syringes connected to the coaxial spinneret. The flow rates in the capillaries were controlled by two separate pumps. Both capillaries were connected to the same high voltage power supply. The electrospun fibers were collected on an aluminum foil placed above the flat grounded metal plate. The applied voltage and the distance between the tip of the spinneret and the collector were maintained at 18 kV and 12 cm, respectively. The shell flow rate was set to 5.0 μL/min, while the core flow rate was varied from 1.0 to 4.0 μL/min. All the electrospinning processes were carried out at around 25 °C and lower than 30% humidity.

2.3. Characterization

Contact-angle measurements using water and iodomethane liquids were carried out for the PLA/CS core/shell non-woven mats, in order to identify possible differences between their wetting abilities. The contact angles were measured using a video contact-angle instrument (Samsung FA-CED camera, Korea), immediately after deionized water was allowed to fall freely onto the surfaces of the flat non-woven mats. The contact angle in each case was taken as the average of five measurements carried out at different locations on the surface of the non-woven mat.

The morphology of the non-woven mats was investigated by FE-SEM (HITACHI S-4700, Japan) with a coating system (BAL-TEC MED020). The average electrospun fiber diameter and its distribution and standard deviation were determined from about 110 fibers measurements from the FE-SEM photographs using visualization software (TOMORO ScopeEye 3.6).

TEM observations (TecnaiG^2, USA) were carried out to determine the core/shell structure of the coaxially electrospun fibers. The samples for the TEM observation were prepared by putting the carbon-coated copper grids on the collector to directly deposit a very thin layer of electrospun fibers on. Then, the copper grids containing fibers without staining was used to take TEM image by passing a beam of electrons through.

The composition of each component in the PLA/CS core/shell composite nanofibers, characterized by their latent heats, was measured by DSC (SH IN2920, TA Instruments, USA). The analyses were carried out at a heating rate of 10 °C/min under a constant stream of nitrogen.

The mechanical performance of the non-woven mats of nanofibers was characterized by a tensile tester (LR 5 K, LLOYD Instrument, UK) with a load cell of 100 N. The electrospun scaffold of each sample was cut into strips in $50 \times 10\,mm^2$ and the dimension of the gauge was 10 mm width by 30 mm length. Its thickness was controlled in range of 100–120 μm by electrospinning time. Each tensile test was operated under a crosshead speed of 5 mm/min and preload of 0.1 MPa at room temperature. All the values of tensile strength and tensile stress represented the average value of 6–7 measurements.

2.4. Antibacterial test

The non-woven mats of the PLA/CS core/shell composite nanofibers were dried under vacuum for 24 h before the antibacterial test was carried out. The antibacterial activity of the PLA/CS core/shell composite nanofibers was evaluated against the common bacterium *Escherichia coli* (Gram negative; ATCC 43895; *E. coli*) using the optical density method (Xie, Liu, & Chen, 2007; Zhao et al., 2003). The bacterial suspension was prepared as follows: 100 μL of bacterial solution containing 10^8 colonies forming per milliliter (CFU/mL) was diluted 10^3 and 10^5 times in Difco nutrient broth solution. A small fragment of the PLA/CS core/shell non-woven mat (approximately 2.0 cm × 3.0 cm and 20 mg) was introduced into 10 mL of the diluted bacterial solution. The mixtures were cultured at 37 °C in a shaking incubator for 24 h. During the incubation, the turbidity of the medium, which represents the growth of bacterial cells, was measured four times at 600 nm with a spectrophotometer (SpectraMax Plus 384, Molecular Devices). The antibacterial efficiency was then calculated from Eq. (1).

$$\text{Antibacterial efficiency} = \left(1 - \frac{OD_2}{OD_1}\right) \times 100, \quad (1)$$

where OD_1 and OD_2 are the measured optical densities of the bacteria in the medium and the bacteria in solution contacting with the PLA/CS core/shell composite nanofibers, respectively, for certain incubation times.

3. Results and discussion

3.1. Morphology of PLA/CS core/shell composite nanofibers

The electrospinning of CS with high molecular weight (690,000 g/mol) was a challenge because of the inherent properties of this material in solution. During electrospinning of CS, the surface tension tends to convert CS solution into drop on the tip of needle. Then, due to multitude of chain entanglements and conformations in CS solution, the drop was ejected into smaller drops and discontinuous fibers, causing blockage at the tip of needle. Meanwhile, it was observed that the insertion of PLA in the core induced the formation of continuous CS nanofibers by coaxial electrospinning. The morphologies of the CS and PLA nanofibers fabricated by single electrospinning and those of PLA/CS composite nanofibers fabricated by coaxial electrospinning are shown in Fig. 1. Different morphologies of nanofibers were observed. It could be seen in Fig. 1(a) that the electrospun CS fibers had heterogeneous morphology composed of many beads and drops among nanofibers. The FE-SEM image of the PLA nanofibers (Fig. 1(b)) shows a fused morphology in which the electrospun fibers are stuck together, whereas a smooth morphology is observed for the coaxially electrospun PLA/CS nanofibers (Fig. 1(c–e)). The average diameter of the PLA/CS core/shell composite nanofibers is much smaller than that of the PLA nanofibers, as shown in Table 1. This is attributed to the different ionic conductivities of the PLA and CS solutions. CS contains amino groups in its molecule, and hence its solution in an acid solvent has higher ionic conductivity. This increases the charge density of the polymer jet during the electrospinning process, and therefore the CS solution is stretched into thinner fibers with smaller diameters than the PLA (Ramakrishna, Teo, Lim, & Ma, 2005).

Table 1
Average diameters of electrospun PLA nanofibers and coaxially electrospun PLA/CS composite nanofibers at different core feed rates. The shell feed rate for coaxial electrospinning was 5.0 μL/min.

Type of sample	Core feed rate (μL/min)	Average diameter (nm)
PLA*	–	736 ± 215
PLA/CS	1.0	236 ± 87
	2.0	303 ± 165
	4.0	396 ± 336

* PLA was electrospun at a feed rate of 5.0 μL/min using a single spinneret. Mean ± standard deviation for $n \geq 110$ fibers.

It can be seen from Table 1 that the average diameter of the coaxially electrospun fibers increases with the increasing feed rate of the core. This is because of the increase in the total amount of fluid jetting out of the coaxial spinneret. The increase in the core feed rate also brings about a broader diameter distribution of the composite nanofibers. The diameters of the coaxial fibers were in the range of 100–700 nm (Fig. 1(c)) and 100–1500 nm (Fig. 1(e)) for core feed rates of 1.0 and 4.0 μL/min, respectively. Similar phenomena have been reported in the fabrication of different core/shell composite nanofibers (Lu et al., 2009; Zhao, Jiang, Pan, Zhu, & Chen, 2007). This is attributed to the instability of the jet caused by the increase in the core feed rate. PLA solution may be separated out from the main jet to form a mixture of PLA nanofibers (large diameter) and PLA/CS core/shell composite nanofibers (small diameter). In general, the diameter differences of five kinds of electrospun fibers were statistically insignificant.

3.2. Core/shell structure of coaxially electrospun PLA/CS composite nanofibers

The flow rate in the electrospinning of polymer solutions is a major variable parameter to be controlled, which can affect the core/shell structure of the composite nanofibers produced (Sun, Duan, & Yuan, 2006). Lower core feed rates lead to the formation of discontinuous core/shell composite nanofibers, whereas the fluid jet is broken into droplets or split into core and shell jets when the core feed rate is over suitable range. In this study, coaxial electrospinning was conducted at a shell feed rate of 5 μL/min, and the core feed rate was varied from 1.0 to 4.0 μL/min. Figs. 2 and 3 show the contact angles for water and iodomethane solvent, respectively, of the non-woven mats of PLA nanofibers and PLA/CS composite nanofibers fabricated at different core feed rates. Contact-angle measurements were employed to confirm the core/shell structure of the PLA/CS composite nanofibers through the difference in the hydrophilic properties of the core and shell materials. Since PLA is highly hydrophobic, its presence in the shell layer of the PLA/CS composite nanofibers causes a decrease in the hydrophilicity of the composite nanofibers. Water (a hydrophilic liquid) and iodomethane (a hydrophobic liquid) were employed for the contact-angle measurements.

The data from the water-contact angle (WCA) measurements (Fig. 2) imply a hydrophobic surface characteristic of the PLA non-woven mat, which showed an average contact-angle of 105.6°. The WCAs of the PLA/CS core/shell non-woven mats, fabricated at core feed rates of 1.0, 2.0, and 4.0 μL/min, were 24.1°, 30.1°, and 52.9°, respectively. It can be seen that the WCA values gradually increased with increasing core feed rate. The following explanation is proposed: when the core feed rate was increased, the amount of CS solution was not sufficient for encapsulation of the PLA solution, causing the solutions of CS and PLA to diffuse into one another

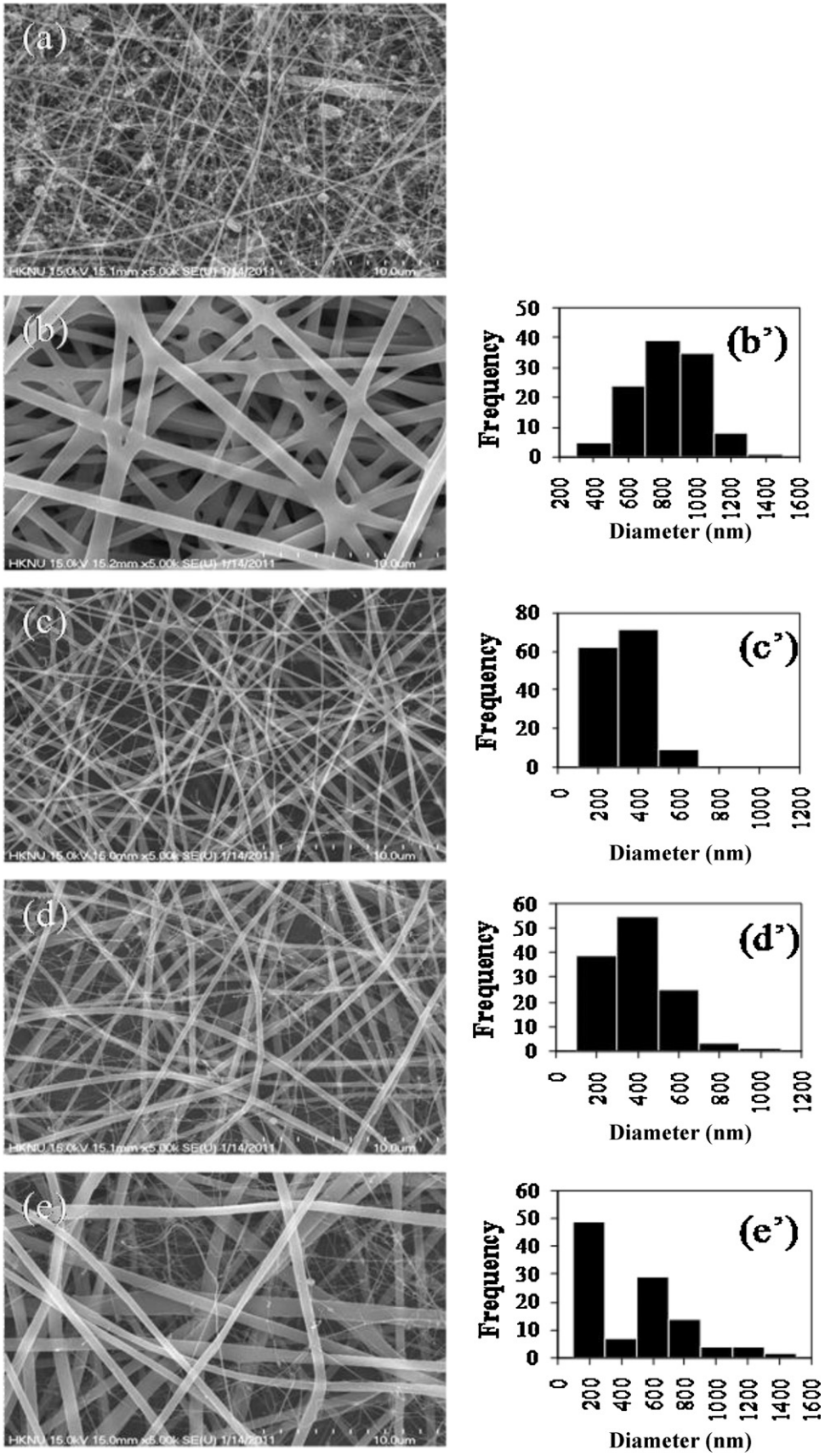

Fig. 1. FE-SEM pictures of (a) the electrospun CS nanofibers, (b) the electrospun PLA nanofibers, and the coaxially electrospun PLA/CS composite nanofibers at sheath feed rate of 5.0 μL/min and core feed rate of (c) 1.0 μL/min, (d) 2.0 μL/min, and (e) 4.0 μL/min. The graphs of (b′), (c′), (d′), and (e′) show the distribution diameter of nanofibers corresponding to (b), (c), (d), and (e), respectively.

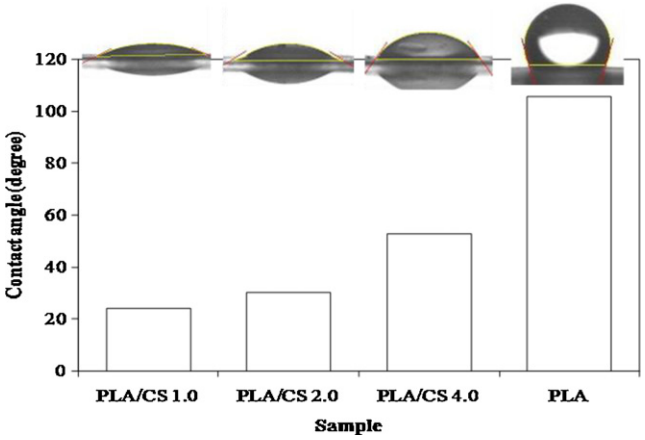

Fig. 2. Water contact angle results of electrospun fibers of the PLA and the PLA/CS coaxially electrospun composite nanofibers fabricated at sheath feed rate of 5.0 μL/min and core feed rate of 1.0 μL/min, 2.0 μL/min and 4.0 μL/min. The inserted pictures show the shapes of the water droplets on the surface of the non-woven mats.

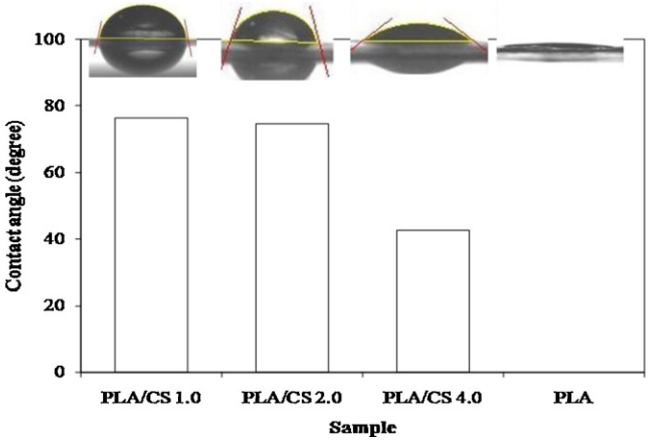

Fig. 3. Iodomethane contact angle results of electrospun fibers of the PLA and the PLA/CS coaxially electrospun fibers fabricated at sheath feed rate of 5.0 μL/min and core feed rate of 1.0 μL/min, 2.0 μL/min and 4.0 μL/min. The inserted pictures show the shapes of the iodomethane droplets on the surface of the non-woven mats.

or to be electrospun separately. The iodomethane contact-angle (ICA) measurements (Fig. 3) show a similar trend to the WCA measurements. When the core feed rates were increased from 1.0 to 4.0 μL/min, the ICA values slowly decreased from 76.3° to 42.6°, indicating that the PLA/CS core/shell non-woven mat was becoming more hydrophobic. At the core feed rate of 4.0 μL/min, there was less probability of the formation of PLA/CS core/shell composite nanofibers.

Fig. 4 shows TEM pictures of the core/shell structures of the PLA/CS composite nanofibers fabricated at the different core feed rates. In TEM observation, the high contrast difference between core and shell was obtained because of the difference between density of core and shell materials. The density of PLA (core) is higher than that of CS (shell), hence fewer electrons are transmitted through the PLA core, leading darker observation. As shown in Fig. 4(a) and (b), the core layer of PLA was completely encapsulated by the outer layer of CS at the core feed rates of 1.0 and 2.0 μL/min. The interface between the core and shell layers is clearly observed. By using a spinneret composed of two coaxial capillaries, two components could be fed through inner and outer coaxial capillary channels and electrospun simultaneously (Díaz, Barrero, Márquez, & Loscertales, 2006; Loscertales et al., 2002). It was reported that when a sufficiently high viscosity of the shell fluid together with a low value of the core/shell interfacial tension were satisfied, a stable Taylor cone was formed at the tip of the needles with an outer meniscus surrounding the inner one. A liquid thread was formed the vertex of each one of the two menisci, resulting in a compound jet of two co-flowing liquids. During travel of the jet to the collector, solvent evaporated and the compound jet solidified to form compound core/shell nanofibers. In this case, the physical properties of the two fluids as well as the liquid flow rates and applied voltages strongly affected on the stability of the structured core/shell nanofibers. The outer layer of the nanofibers became thinner when the core feed rate was changed from 1.0 to 2.0 μL/min. When the core feed rate was increased to 4.0 μL/min, bi-component nanofibers were formed side by side (Fig. 4(c)), rather than the core/shell structure of composite nanofibers. This

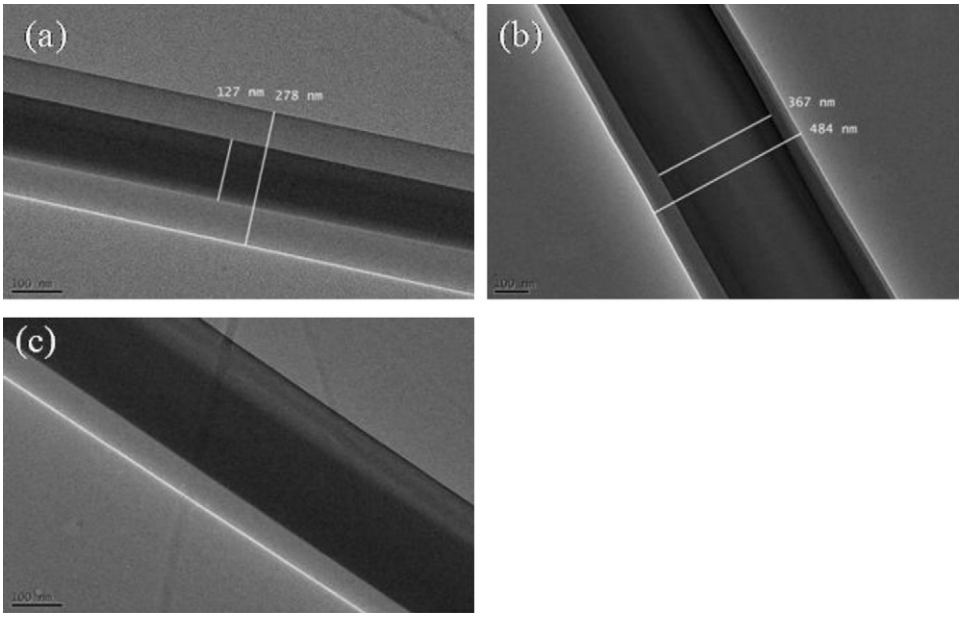

Fig. 4. TEM pictures of the coaxially electrospun composite nanofibers of the PLA/CS fabricated at shell feed rate of 5.0 μL/min and core feed rate of (a) 1.0 μL/min, (b) 2.0 μL/min and (c) 4.0 μL/min.

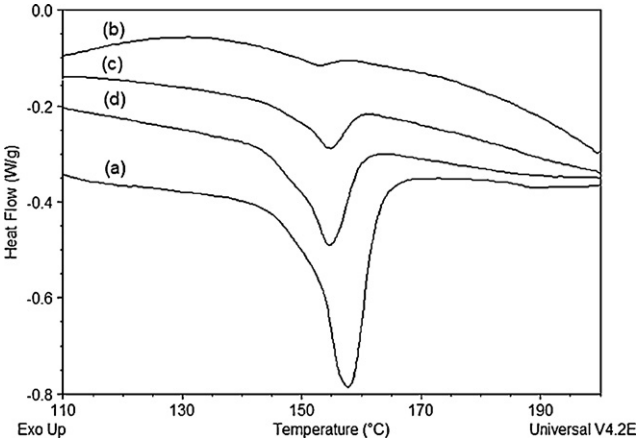

Fig. 5. DSC results of (a) the PLA nanofibers and the PLA/CS core/shell composite nanofibers fabricated at shell feed rate of 5.0 μL/min and core feed rate of (b) 1.0 μL/min, (c) 2.0 μL/min, and (d) 4.0 μL/min.

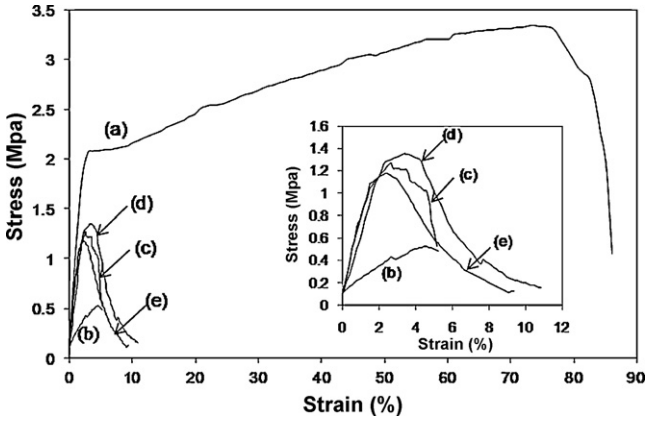

Fig. 6. Tensile test results of non-woven mats of (a) the PLA nanofibers, (b) the CS nanofibers, and the PLA/CS core/shell composite nanofibers fabricated at shell feed rate of 5.0 μL/min and core feed rate of (c) 1.0 μL/min, (d) 2.0 μL/min, and (e) 4.0 μL/min.

formation of an incomplete core/shell structure at the core feed rate of 4.0 μL/min is attributed to the insufficient amount of shell solution and the instability of the primary jet, leading to axial anisotropy of core/shell fluids.

3.3. PLA content in PLA/CS core/shell composite nanofibers

PLA is a crystalline polymer, whereas CS is not. Owing to the morphology differences between PLA and CS, the analysis for the individual PLA and CS component proportion in PLA/CS core/shell composite nanofibers was carried out by DSC method. The DSC thermograms of the non-woven mats of PLA nanofibers and PLA/CS core/shell composite nanofibers, fabricated at different core feed rates, are shown in Fig. 5. Table 2 summarizes the melting points, heats of fusion, and percentages of PLA in the core for the PLA/CS core/shell composite nanofibers. The PLA nanofibers had a melting point of 157.8 °C, which was higher than that of the electrospun PLA/CS core/shell composite nanofibers. This difference is attributed to the presence of CS, an amorphous polymer, affecting the melting of the PLA. When the core feed rates were increased, the heat of fusion of the PLA/CS core/shell composite nanofibers increased. At the same time, their endothermic curves became bigger and sharper, implying a higher content of PLA in the PLA/CS core/shell composite nanofibers. On the basis of the heats of fusion of the PLA and PLA/CS core/shell composite nanofibers, the approximate percentage of PLA in the core layer can be calculated from Eq. (2)

$$\text{Percentage of PLA} = \frac{\Delta H_{\text{PLA/CS}}}{\Delta H_{\text{PLA}}} \times 100, \quad (2)$$

where $\Delta H_{\text{PLA/CS}}$ and ΔH_{PLA} are the measured heats of fusion of the PLA/CS core/shell composite nanofibers and PLA nanofibers, respectively.

It can be seen from Table 2 that when the core feed rate was 1.0 μL/min, the content of PLA in the core/shell composite nanofibers was small (3.9 wt%) compared with that of CS. However, when the core feed rate reached 4.0 μL/min, PLA became the predominant constituent (61.4 wt%), and could not be completely encapsulated by CS. This analysis is consistent with the above TEM results.

3.4. Mechanical properties of coaxially electrospun PLA/CS core/shell composite nanofibers

The stress–strain curves of the electrospun non-woven mats of PLA nanofibers and PLA/CS core/shell composite nanofibers fabricated at different core feed rates are shown in Fig. 6. The results indicate that the non-woven mat of PLA nanofibers had a high tensile stress of 3.3 MPa, with a tensile strain of 86.1%. Electrospun CS nanofibers had poor mechanical strength (0.5 MPa and 5.2%), hence it was expected that the encapsulation of PLA in the core of the composite nanofibers might increase its tensile strength. The stress–strain curves of the PLA/CS core/shell composite nanofibers made with different core feed rates showed similar trends. Because of introduction of the PLA component, the tensile strength of PLA/CS core/shell composite nanofibers were significantly improved with respect to the electrospun CS nanofibers. The tensile stress and tensile strain of the composite nanofibers made at a core feed rate of 2.0 μL/min were 1.4 MPa and 10.9%, respectively. However, the non-woven mat of PLA/CS core/shell composite nanofibers fabricated at a core feed rate of 4.0 μL/min showed lower tensile strength, although it contained higher amount of PLA component. This is attributed to the poor core/shell structure, in which the PLA component is not only contributed on the core but also on the surface of electrospun nanofibers, as confirmed by the contact-angle measurements and TEM results. It was supposed that increasing in the amount of PLA in core to 61 wt% could not increase mechanical properties of composite nanofibers which did not possess core/shell structure.

Table 2
Thermal properties and percentages of PLA in the core of PLA/CS core/shell composite nanofibers fabricated at different core feed rates.

Type of sample	Core feed rate (μL/min)	Melting temperature (T_m, °C)	Heat of fusion (ΔH_m, J/g)	Percentage of PLA (%) in core
PLA*	–	157.8	30.7	100
	1.0	152.2	1.19	3.9
PLA/CS	2.0	154.5	7.03	22.9
	4.0	154.5	18.9	61.4

* PLA was electrospun at a feed rate of 5.0 μL/min using a single spinneret.

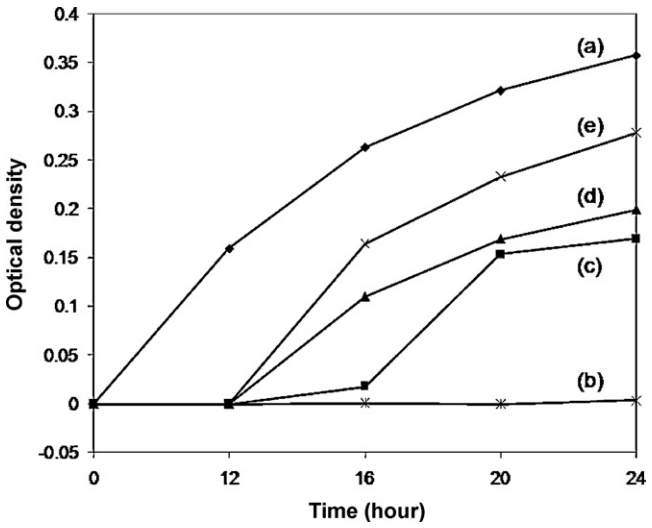

Fig. 7. The curves of OD as function of time for (a) medium, (b) CS cast film and non-woven mat of the PLA/CS core/shell composite nanofibers fabricated at shell feed rate of 5.0 μL/min and core feed rate of (c) 1.0 μL/min, (d) 2.0 μL/min, and (e) 4.0 μL/min. All solutions initially contained approximately 10^5 CFU/mL of *E. coli* before incubation.

3.5. Antibacterial activity of electrospun PLA/CS core/shell composite nanofibers

CS has a marked ability to inhibit the growth of a number of Gram positive and Gram negative bacteria (Chen, Wu, & Zeng, 2005; Chung, Wang, Chen, & Li, 2003; Helander, Nurmiaho-Lassila, Ahvenainen, Rhoades, & Roller, 2001; Liu et al., 2006). This compound is known to either bind or modify minerals that are important for microbial growth, or impair membrane function and inhibit bacterial replication by interacting with the cell membrane. Its inhibitory effect varies with its degree of deacetylation and molecular weight, and with the pH of the medium. Two concentrations of *E. coli* bacterial solution, containing approximately 10^3 and 10^5 CFU/mL, were used to test the antibacterial activity of the PLA/CS core/shell composite nanofibers. Fig. 7 shows the optical density (OD) curves as a function of incubation time for the medium containing approximately 10^5 CFU/mL and PLA/CS core/shell composite nanofibers. Since bacterial cells are opaque, bacterial propagation can be evaluated by the turbidity of the solution; a lower OD value of the bacterial solution means less propagation. The growth rate of the bacteria in the solution was obtained by measuring the OD of the solution after certain incubation periods.

As shown in Fig. 7, all the non-woven mats of PLA/CS core/shell composite nanofibers completely inhibited the growth of bacteria for the first 12 h, and after this time, the bacteria gradually grew. However, the concentrations of bacteria in solutions in contact with the PLA/CS core/shell composite nanofibers were lower than that of bacteria in the medium, exhibiting the antibacterial activity of CS. The CS cast film showed the highest efficiency for *E. coli* inhibition (99%). This CS cast film was observed to be completely dissolved in the bacterial solution during the test. This phenomenon might significantly induce the contact between CS molecules and bacterial cells, leading to the high antibacterial activity. When the core feed rate increased from 1.0 μL/min to 2.0 and 4.0 μL/min, the efficiency of *E. coli* inhibition was found to decrease from 52% to 44% and 22%, respectively. This can be explained as follows: the nanofibers fabricated by coaxial electrospinning at a core feed rate of 4.0 μL/min are a blend of PLA and CS, so the CS, as the active component for antibacterial activity, is found not only on the surface, but also inside the nanofibers, resulting in less contact between CS molecules and bacterial cells. At a core feed rate of 1.0 μL/min, the PLA/CS core/shell composite nanofibers provided stable antibacterial activity with an efficiency of 52% after 24 h. When the core feed rate was 2.0 μL/min, the coaxially electrospun non-woven mat might contain not only core/shell but also few blend nanofibers, leading to decrease of antibacterial efficiency. At the lower concentration of bacteria (10^3 CFU/mL), the PLA/CS core/shell composite nanofibers exhibited significant antibacterial activity. In this case, the OD value of the bacterial solution in contact with the non-woven mat of PLA/CS core/shell composite nanofibers (fabricated at core feed rate of 1.0 μL/min) was unchanged after 24 h, implying an antibacterial efficiency of 100%. With the increase in core feed rate from 2.0 to 4.0 μL/min, the antibacterial efficiency decreased from 99.6 to 99.2%.

In developing an antibacterial, several criteria must be considered. First, the materials should possess a good effectiveness (defined as 30% decrease of a microbial concentration over a time provided by sufficient amount of agent). Second, a long term antibacterial activity is desired to achieve long lasting protection against bacteria. Finally, the materials are supposed to be easily handled and non-toxic to human being. The composite material containing coaxially electrospun PLA/CS fibers can satisfy these criteria. In addition, CS has biocompatibility and wound healing properties, making it good candidate for biomedical application such as wound dressing as a barrier to bacteria (Jayakumar et al., 2011).

4. Conclusion

PLA/CS composite nanofibers were successfully fabricated by the coaxial electrospinning process. The composite nanofibers formed at a core feed rate of 2 μL/min had an average diameter of 303 nm with a double-layer structure, in which PLA and CS formed the core and shell layers, respectively. The effects of the core feed rate on the core/shell structure and morphology of the nanofibers were studied using SEM, TEM, and contact-angle analysis. The results indicated that a uniform core/shell structure and fine morphology of the PLA/CS composite nanofibers were obtained at core feed rates of 1.0 and 2.0 μL/min with a shell feed rate of 5.0 μL/min. The PLA/CS core/shell composite nanofibers exhibited antibacterial activity against *E. coli*. The composite nanofibers fabricated at a core feed rate of 1.0 μL/min had the highest antibacterial efficiency of 100% and 52% for bacterial concentrations of 10^3 and 10^5 CFU/mL, respectively. This high antibacterial activity means that these PLA/CS core/shell composite nanofibers have a high potential for applications in biomedical fields.

References

Bhardwaj, N., & Kundu, S. C. (2010). Electrospinning: A fascinating fiber fabrication technique. *Biotechnology Advances*, *28*, 325–347.

Chen, S., Wu, G., & Zeng, H. (2005). Preparation of high antimicrobial activity thiourea chitosan-Ag^+ complex. *Carbohydrate Polymers*, *60*, 33–38.

Chronakis, I. S. (2005). Novel nanocomposites and nanoceramics based on polymer nanofibers using electrospinning process—A review. *Journal of Materials Processing Technology*, *167*, 283–293.

Chung, Y.-C., Wang, H.-L., Chen, Y.-M., & Li, S.-L. (2003). Effect of abiotic factors on the antibacterial activity of chitosan against waterborne pathogens. *Bioresource Technology*, *88*, 179–184.

Díaz, J. E., Barrero, A., Márquez, M., & Loscertales, I. G. (2006). Controlled encapsulation of hydrophobic liquids in hydrophilic polymer nanofibers by co-electrospinning. *Advanced Functional Materials*, *16*, 2110–2116.

Frenot, A., & Chronakis, I. S. (2003). Polymer nanofibers assembled by electrospinning. *Current Opinion in Colloid & Interface Science*, *8*, 64–75.

Geng, X., Kwon, O.-H., & Jang, J. (2005). Electrospinning of chitosan dissolved in concentrated acetic acid solution. *Biomaterials*, *26*, 5427–5432.

He, C.-L., Huang, Z.-M., & Han, X.-J. (2009). Fabrication of drug-loaded electrospun aligned fibrous threads for suture applications. *Journal of Biomedical Materials Research Part A*, *89A*, 80–95.

Helander, I. M., Nurmiaho-Lassila, E. L., Ahvenainen, R., Rhoades, J., & Roller, S. (2001). Chitosan disrupts the barrier properties of the outer membrane of Gram-negative bacteria. *International Journal of Food Microbiology*, *71*, 235–244.

Homayoni, H., Ravandi, S. A. H., & Valizadeh, M. (2009). Electrospinning of chitosan nanofibers: Processing optimization. *Carbohydrate Polymers*, *77*, 656–661.

Huang, Z.-M., Zhang, Y., & Ramakrishna, S. (2005). Double-layered composite nanofibers and their mechanical performance. *Journal of Polymer Science Part B: Polymer Physics*, *43*, 2852–2861.

Jayakumar, R., Prabaharan, M., Sudheesh Kumar, P. T., Nair, S. V., & Tamura, H. (2011). Biomaterials based on chitin and chitosan in wound dressing applications. *Biotechnology Advances*, *29*, 322–337.

Ji, W., Yang, F., van den Beucken, J. J. J. P., Bian, Z., Fan, M., Chen, Z., et al. (2010). Fibrous scaffolds loaded with protein prepared by blend or coaxial electrospinning. *Acta Biomaterialia*, *6*, 4199–4207.

Jia, Y.-T., Gong, J., Gu, X.-H., Kim, H.-Y., Dong, J., & Shen, X.-Y. (2007). Fabrication and characterization of poly(vinyl alcohol)/chitosan blend nanofibers produced by electrospinning method. *Carbohydrate Polymers*, *67*, 403–409.

Jiang, H., Hu, Y., Li, Y., Zhao, P., Zhu, K., & Chen, W. (2005). A facile technique to prepare biodegradable coaxial electrospun nanofibers for controlled release of bioactive agents. *Journal of Controlled Release*, *108*, 237–243.

Jiang, H., Hu, Y., Zhao, P., Li, Y., & Zhu, K. (2006). Modulation of protein release from biodegradable core-shell structured fibers prepared by coaxial electrospinning. *Journal of Biomedical Materials Research Part B: Applied Biomaterials*, *79B*, 50–57.

Liang, D., Hsiao, B. S., & Chu, B. (2007). Functional electrospun nanofibrous scaffolds for biomedical applications. *Advanced Drug Delivery Reviews*, *59*, 1392–1412.

Liu, N., Chen, X.-G., Park, H.-J., Liu, C.-G., Liu, C.-S., Meng, X.-H., et al. (2006). Effect of MW and concentration of chitosan on antibacterial activity of *Escherichia coli*. *Carbohydrate Polymers*, *64*, 60–65.

Loscertales, I. G., Barrero, A., Guerrero, I., Cortijo, R., Marquez, M., & Gañán-Calvo, A. M. (2002). Micro/nano encapsulation via electrified coaxial liquid jets. *Science*, *295*, 1695–1698.

Lu, Y., Jiang, H., Tu, K., & Wang, L. (2009). Mild immobilization of diverse macromolecular bioactive agents onto multifunctional fibrous membranes prepared by coaxial electrospinning. *Acta Biomaterialia*, *5*, 1562–1574.

Ohkawa, K., Cha, D., Kim, H., Nishida, A., & Yamamoto, H. (2004). Electrospinning of chitosan. *Macromolecular Rapid Communications*, *25*, 1600–1605.

Pillai, C. K. S., Paul, W., & Sharma, C. P. (2009). Chitin and chitosan polymers: Chemistry, solubility and fiber formation. *Progress in Polymer Science*, *34*, 641–678.

Ramarkrishna, K. F., Teo, W.-E., Lim, T.-C., & Ma, Z. (2005). *An introduction to electrospinning and nanofibers* (1st ed.). Singapore: World Scientific Publishing.

Rutledge, G. C., & Fridrikh, S. V. (2007). Formation of fibers by electrospinning. *Advanced Drug Delivery Reviews*, *59*, 1384–1391.

Shalumon, K. T., Anulekha, K. H., Girish, C. M., Prasanth, R., Nair, S. V., & Jayakumar, R. (2010). Single step electrospinning of chitosan/poly(caprolactone) nanofibers using formic acid/acetone solvent mixture. *Carbohydrate Polymers*, *80*, 413–419.

Shih, C.-M., Shieh, Y.-T., & Twu, Y.-K. (2009). Preparation and characterization of cellulose/chitosan blend films. *Carbohydrate Polymers*, *78*, 169–174.

Sill, T. J., & von Recum, H. A. (2008). Electrospinning: Applications in drug delivery and tissue engineering. *Biomaterials*, *29*, 1989–2006.

Sun, B., Duan, B., & Yuan, X. (2006). Preparation of core/shell PVP/PLA ultrafine fibers by coaxial electrospinning. *Journal of Applied Polymer Science*, *102*, 39–45.

Sun, Z., Zussman, E., Yarin, A. L., Wendorff, J. H., & Greiner, A. (2003). Compound core-shell polymer nanofibers by co-electrospinning. *Advanced Materials*, *15*, 1929–1932.

Torres-Giner, S., Ocio, M. J., & Lagaron, J. M. (2008). Development of active antimicrobial fiber-based chitosan polysaccharide nanostructures using electrospinning. *Engineering in Life Sciences*, *8*, 303–314.

Torres-Giner, S., Ocio, M. J., & Lagaron, J. M. (2009). Novel antimicrobial ultrathin structures of zein/chitosan blends obtained by electrospinning. *Carbohydrate Polymers*, *77*, 261–266.

Wang, C.-C., & Chen, C.-C. (2005). Anti-bacterial and swelling properties of acrylic acid grafted and collagen/chitosan immobilized polypropylene non-woven fabrics. *Journal of Applied Polymer Science*, *98*, 391–400.

Xiaoqiang, L., Yan, S., Rui, C., Chuanglong, H., Hongsheng, W., & Xiumei, M. (2009). Fabrication and properties of core-shell structure P(LLA-CL) nanofibers by coaxial electrospinning. *Journal of Applied Polymer Science*, *111*, 1564–1570.

Xie, Y., Liu, X., & Chen, Q. (2007). Synthesis and characterization of water-soluble chitosan derivate and its antibacterial activity. *Carbohydrate Polymers*, *69*, 142–147.

Xie, J., Li, X., & Xia, Y. (2008). Putting electrospun nanofibers to work for biomedical research. *Macromolecular Rapid Communications*, *29*, 1775–1792.

Xu, J., Zhang, J., Gao, W., Liang, H., Wang, H., & Li, J. (2009). Preparation of chitosan/PLA blend micro/nanofibers by electrospinning. *Materials Letters*, *63*, 658–660.

Yi, F., & LaVan, D. A. (2008). Poly(glycerol sebacate) nanofiber scaffolds by core/shell electrospinning. *Macromolecular Bioscience*, *8*, 803–806.

Zhang, H., Li, S., Branford White, C. J., Ning, X., Nie, H., & Zhu, L. (2009). Studies on electrospun nylon-6/chitosan complex nanofiber interactions. *Electrochimica Acta*, *54*, 5739–5745.

Zhang, Y. Z., Wang, X., Feng, Y., Li, J., Lim, C. T., & Ramakrishna, S. (2006). Coaxial electrospinning of (fluorescein isothiocyanate-conjugated bovine serum albumin)-encapsulated poly(∈-caprolactone) nanofibers for sustained release. *Biomacromolecules*, *7*, 1049–1057.

Zhao, L., Mitomo, H., Zhai, M., Yoshii, F., Nagasawa, N., & Kume, T. (2003). Synthesis of antibacterial PVA/CM-chitosan blend hydrogels with electron beam irradiation. *Carbohydrate Polymers*, *53*, 439–446.

Zhao, P., Jiang, H., Pan, H., Zhu, K., & Chen, W. (2007). Biodegradable fibrous scaffolds composed of gelatin coated poly(∈-caprolactone) prepared by coaxial electrospinning. *Journal of Biomedical Materials Research Part A*, *83A*, 372–382.